Cryogenic Engineering
Conference
Ann Arbor, Michigan, 8/15/61

GAS REQUIREMENTS IN PRESSURIZED TRANSFER OF LIQUID HYDROGEN

D. F. Gluck and J. F. Kline

Lewis Research Center
National Aeronautics and Space Administration
Cleveland, Ohio

Introduction

Of late, liquid hydrogen has become a very popular fuel for space missions. It is being used in such programs as Centaur and Saturn. Furthermore, hydrogen is the ideal working fluid for nuclear powered space vehicles currently under development. In these applications, liquid hydrogen fuel is generally transferred to the combustion chamber by a combination of pumping and pressurization. The pump forces the liquid propellant from the fuel tank to the combustion chamber; gaseous pressurant holds tank pressure sufficiently high to prevent cavitation at the pump inlet and to maintain the structural rigidity of the tank.

The pressurizing system, composed of pressurant, tankage, and associated hardware can be a large portion of the total vehicle weight. Pressurant weight can be reduced by introducing the pressurizing gas at temperatures substantially greater than those of liquid hydrogen. Heat and mass transfer processes thereby induced complicate gas requirements during discharge. These requirements must be known to insure proper design of the pressurizing system.

The aim of this paper is to develop from basic mass and energy transfer processes a general method to predict helium and hydrogen gas usage for the pressurized transfer of liquid hydrogen. This required an analytical and experimental investigation, the results of which are described in this paper.

Analysis

BASIC RELATIONS. Figure 1 shows a schematic of the discharge from a cylindrical tank as considered in this analysis. The initial ullage volume, V_o, is rapidly pressurized to the desired discharge pressure, P. Thereupon, discharge is started, inlet gas displacing liquid hydrogen until the tank is nearly emptied (ullage volume now equal to V_f). The initial ullage volume is generally small, about 10-15% of the total volume.

This analysis is concerned only with predicting the gas required to discharge the tank (as opposed to the gas required to pressurize the initial ullage volume). This gas usage is not simply a matter of displaced volumes, since the entering inlet gas is cooled on contact with the colder tank walls and dome. Furthermore, mass transfer may occur at the gas-liquid interface. These processes can be related to the gas requirements through a gas phase energy balance as shown in Figure 2. The changing volume gas phase (enclosed by the dashed lines) is chosen as the thermodynamic system.

Within a differential of discharge time, $d\varphi$, the following energy processes occur (all symbols defined in nomenclature):

(1) enthalpy is carried into the system by the pressurizing gas, $h_i\ dm$;

(2) the entire gas phase experiences an internal energy change, dU;

(3) flow work is done in extending the system boundary $(P/J)\,dV$;

(4) enthalpy is lost from the system by mass transfer at the interface, $h_s\ dm_t$;

(5) there is heat transfer from the gas phase to the surroundings, dQ.

A differential energy balance for the whole gas phase can therefore be written as

$$h_i\ dm - \left[dU + \frac{1}{J} P\ dV + h_s\ dm_t + dQ\right] = 0 \qquad (1)$$

From the definition of enthalpy

$$dH = dU + \frac{1}{J}[d(PV)] \tag{2}$$

and, since for a constant pressure process

$$d(PV) = P\,dV \tag{3}$$

there obtains from equations (1), (2), and (3) that

$$h_i\,dm - [dH + h_s\,dm_t + dQ] = 0 \tag{4}$$

Since both h_i and h_s are essentially constant (inlet gas temperature and hydrogen saturation temperature are constant), equation (4) can be integrated over the entire time of discharge to give

$$h_i\,\Delta m - [\Delta H + h_s m_t + Q] = 0 \tag{5}$$

This can be rearranged to yield the gas required to effect discharge

$$\Delta m = \frac{\Delta H + h_s m_t + Q}{h_i} \tag{6}$$

Thus, for a given gas inlet temperature (determines h_i) and liquid discharge pressure (determines h_s), the problem of predicting Δm, the gas required for discharge, is simplified to that of predicting the more basic terms ΔH, m_t, and Q. First, the change of gas phase enthalpy, ΔH, will be considered.

GAS PHASE ENTHALPY CHANGE. A theoretical expression for gas phase enthalpy change can readily be determined if the gas in the ullage volume can be considered as an ideal, constant-specific-heat gas within the temperature ranges involved. At temperature T within this range, the specific enthalpy can be written as

$$h = h_R + C_p(T - T_R) \tag{7}$$

Since the lowest temperature the gas is likely to attain is the saturation temperature of the liquid hydrogen, the saturation state (constant during discharge)

can be taken as the reference value for equation (7). Thus

$$h = h_s + C_p(T - T_s) \tag{8}$$

Inasmuch as the ullage volume is a non-isothermal region, the total gas phase mass and enthalpy are given respectively by

$$m = \int_o^V \rho \, dV \tag{9}$$

and

$$H = \int_o^V h\rho \, dV \tag{10}$$

Combining equations(8), (9), and (10),

$$H = (h_s - C_pT_s)m + C_p \int_o^V T\rho \, dV \tag{11}$$

Substitution of the ideal gas relation

$$T\rho = \frac{MP}{R} \tag{12}$$

and integration at constant pressure then yields

$$H = (h_s - C_pT_s)m + \left(\frac{C_pMP}{R}\right) V \tag{13}$$

The change in gas phase total enthalpy during discharge (from original to final volume) is then

$$\Delta H \equiv H_f - H_o = (h_s - C_pT_s)(m_f - m_o) + \left(\frac{C_pM}{R}\right) P \, \Delta V \tag{14}$$

Now from conservation of mass

$$m_o + \Delta m = m_f + m_t \tag{15}$$

so that, finally

$$\Delta H = (h_s - C_pT_s)(\Delta m - m_t) + \left(\frac{C_pM}{R}\right) P \, \Delta V \tag{16}$$

Substitution of equation (16) into equation (6) then yields for the gas mass

$$\Delta m = \frac{(C_p M/R) P \, \Delta V}{(h_i - h_s) + C_p T_s} + \frac{C_p T_s m_t}{(h_i - h_s) + C_p T_s} + \frac{Q}{(h_i - h_s) + C_p T_s} \qquad (17)$$

In equation (17) the first term on the right hand side represents the mass required to merely displace the liquid, the second term is that required because of interfacial mass transfer, and the third represents the mass required to counteract heat loss. As C_p, M, and R are properties of the pressurant and P, ΔV, h_i, and h_s are obtained from prescribed operating conditions, the problem is now reduced to determining m_t and Q.

INTERFACIAL MASS TRANSFER. Mass can be transferred across the liquid hydrogen interface by means of condensation or evaporation. There is evidence that the condition of the liquid interface markedly influences gas-liquid mass transfer. Interfacial mass transfer might be of particular significance in systems in which the interface is agitated by tank vibration.

During pressurization with hydrogen gas, the liquid hydrogen is subcooled. This results in rapid condensation of hydrogen at the interface, quickly raising the interface temperature to the saturation temperature corresponding to tank pressure. Thereafter, the rate of condensation is set by the rate of heat transfer from the interface to the colder liquid. Clark (ref. 1), assuming that this heat transfer process was similar to transient heat conduction into a semi-infinite slab, estimated that gaseous condensation was negligibly small. However, this theory has not received adequate experimental confirmation.

When helium pressurant is used on hydrogen liquid, the complication of a two component system is encountered. Because of the complexity of this system, an analysis not contingent upon restrictive or unrealistic assumptions did not

seem possible. It was felt desirable, therefore, to obtain an experimental evaluation of the general magnitude of the interfacial mass transfer term of equation (17) for hydrogen and helium pressurants, and to ascertain its significance compared to the other two terms.

HEAT TRANSFER. Heat transfer takes place from the gas to the tank piping and inlet diffuser, the tank dome, and the tank walls. In general, it is expected that heat transfer to the tank wall, Q_w, will be the dominant factor in the heat transfer. It is therefore convenient to express the total heat transfer as

$$Q = Q_w + Q_e \tag{18}$$

where Q_e is the heat input to the components (piping, screens, and dome) in the upper end of the tank. The development of a prediction technique for end heat transfer is difficult to achieve since this heat input will depend on the particular tank and piping design, dome geometry, etc. However, the wall heat transfer is amenable to analysis.

The theoretical method developed by Clark (ref. 2) for calculating wall heat transfer could not be applied to liquid hydrogen discharges, as the requirements of constant gas and wall properties cannot generally be met. Under conditions encountered in a single hydrogen discharge, gas density can vary 10 fold and wall specific heat 100 fold. Therefore an alternate approach, dimensional analysis, was used. It was hoped in this way to develop a relatively simple empirical wall heat transfer correlation.

Preliminary data and theoretical considerations indicated that the heat transferred to the side walls of a cylindrical tank, Q_w, can be expressed as a function of the following variables

$$Q_w = f(\mathcal{H}, \theta, C, C_w, D, L, Q_{w,\infty}) \tag{19}$$

where the gas phase and wall thermal capacities (per unit wall area) are respectively

$$C = \bar{C}_p \bar{\rho} D \tag{20}$$

and

$$C_w = \bar{C}_{p,w} \rho_w \delta \tag{21}$$

The term $Q_{w,\infty}$ is the heat transferred to the wall if the entire wall were heated to the temperature of the inlet gas,

$$Q_{w,\infty} = \pi \rho_w D L \delta \int_{T_s}^{T_i} C_{p,w} \, dT \tag{22}$$

From equation (19) the following dimensionless equation results

$$\frac{Q_w}{Q_{w,\infty}} = \Phi \left[\left(\frac{C}{C_w} \right) \left(\frac{\mathcal{H}\theta}{C_w} \right) \left(\frac{L}{D} \right) \right] \tag{23}$$

The group $Q_w/Q_{w,\infty}$ is the fractional approach to the total possible heat transfer. The groups C/C_w and $\mathcal{H}\theta/C_w$ represent the tendency for the wall to become heated. The former expresses wall response to gas phase temperature potential; the latter expresses wall response to the heat transfer coefficient and discharge time. The final group, L/D, is a reflection of the fraction of the gas involved in the wall heat transfer process. Experimental work is needed to determine the function Φ of equation (23).

If the proposed heat transfer correlation proves feasible, the working relation for gas requirement will be given from equations (17), (18), and (23), as

$$\Delta m = \frac{1}{(h_i - h_s) + C_p T_s} \left[\left(\frac{C_p M}{R} \right) P \, \Delta V + C_p T_s m_t + \Phi Q_{w,\infty} + Q_e \right] \tag{24}$$

Experimental Set-up

An experimental investigation of liquid hydrogen discharge with gas pressurant was made to study the phenomenon and to evaluate the unknown parameters and functional relations of equation (24). It was also desired to experimentally test the theoretically-derived equation (16) upon which equation (24) depends. A brief summary of the apparatus, instrumentation, and test procedures used and the major results of the tests will now be given.

APPARATUS. Expulsion conditions were studied using a 27-inch diameter cylindrical tank with dished head ends, 89 inches long overall, made of 5/16 inch thick 304 stainless steel plate. Heat leak to the tank was controlled by a vacuum jacket surrounding the entire tank. An isometric view of the tank is shown in Figure 3.

The inlet gas diffuser, which was overdesigned to insure that flow was directed vertically downward with a flat velocity profile, occupied the entire upper end. The diffuser and the instrumentation in the upper end of the tank are shown in figure 4. The inner surface of the tank dome was insulated with a 1/2-inch layer of cork, and the diffuser parts and screens were made thin in order to minimize cooling of the incoming gas.

The cylindrical portion of the tank was left clear (no slosh baffles, ribs, etc.) to avoid artificial disturbance of the liquid or gas during outflow. The liquid outlet was centered in the bottom surface and no vortex spoiler was installed.

Either hydrogen or helium pressurizing gas was available from supply cylinders. The gas was drawn from parallel pressurizing systems and passed through a flow rate measuring orifice before entering the tank.

INSTRUMENTATION. Liquid and gas temperatures inside the tank were sensed with fixed semiconductor (carbon resistor) probes. Through selection, ageing and calibration, an absolute accuracy better than $\pm 0.2^{\circ}$ R at 37° R was indicated (ref. 3). A vertical survey was made at the mid-radius position with probes spaced 1/3 inch apart. A transverse survey was made at the 50% ullage level with 1/4 inch spacing near the wall. Specific fluid temperature measuring locations are indicated by the solid dots in Figure 3.

Metal temperatures were sensed with copper-constantan thermocouples soldered directly to the outer surface of the tank wall. These thermocouple locactions are also indicated in figure 3 by the triangles on the tank wall.

Probe signals were sampled at the rate of 18 per second, so that any particular temperature profile was surveyed in about $1\frac{1}{2}$ seconds.

PROCEDURE. Each expulsion trial began with the tank filled to within 6 inches of the diffuser outlet screen (15% ullage) with liquid para-hydrogen boiling at atmospheric pressure, and all metal temperatures stabilized. The tank was pressurized within 10 seconds, and liquid outflow was initiated and stabilized within 10 seconds. Gas was continually supplied to keep the ullage pressure constant. The outflow rate was held constant.

Ten experimental runs were made using ambient temperature hydrogen or helium as pressurant. Nominal liquid outflow rates were 0.3 and 1.0 lb/sec and tank pressures were 60 and 160 psia. Heat leak from the ambient surroundings was low, generally about 40 Btu/hr-sq ft.

Results and Discussion

The operating conditions, major results, and measured and calculated quantities of interest obtained from the test runs are summarized in table 1 and discussed in the following sections.

INTERFACIAL MASS TRANSFER. A gas phase inventory method was used to determine the quantity of interfacial mass transfer, m_t, from the experimental data. In this method, the quantity of gas in the tank after discharge is compared to the quantity originally present plus that added during discharge. This may be expressed mathematically as

$$m_t = m_f - (\Delta m + m_o) \tag{25}$$

The gas added during discharge, Δm, was determined from supply cylinder temperature and pressure before and after discharge. These quantities were corroborated by integration of orifice gas flow rates.

The original mass of ullage gas m_o and the final mass m_f were evaluated by numerically integrating the experimental gas density profile throughout the respective gas phase volumes according to equation (9). Values for gas density in these integrations were obtained from real gas property data at the tank pressure and local gas temperature. Hydrogen gas state data were obtained from reference 4 and helium gas density was obtained using the Beattie-Bridgeman equation.

For the hydrogen pressurized discharges, it was found in all the runs that the type of mass transfer encountered was evaporation rather than condensation. Of the gas added during discharge, the percent transferred was 2.8% on the average and 7.8% in the extreme case (column 7 of table 1).

For helium pressurized discharges, it was assumed that the helium compressed the hydrogen gas initially in the tank into a layer above the liquid. The tank therefore was assumed to consist of three zones: liquid hydrogen, vaporous hydrogen, and gaseous helium. A mass inventory was carried out similarly to that just described for the one component system, with the difference that in the calculation of m_o and m_f, allowance was made for the two gas zones.

The results showed that in some runs, condensation of hydrogen vapor, and in others evaporation of liquid hydrogen, occurred. In two runs, the calculations indicated that helium dissolved in the liquid hydrogen. In no run did the calculated mass transfer exceed 12% of the pressurant usage (column 7 of table 1). It was believed that these rather erratic results were due to the assumption of gas phase stratification. The magnitudes of the mass transfer calculated for helium was therefore considered somewhat questionable.

ENTHALPY CHANGE. In the development of the equation for enthalpy change (eq. (16)), it was assumed that the gas in the ullage volume can be represented by the ideal gas equation of state and has a constant specific heat for the temperature range T_s to T_i. In order to obtain an indication of the validity of equation (16) a comparison was made of values of ΔH calculated using equation (16) and those obtained from experimental gas phase data. In evaluating ΔH from equation (16), experimentally determined values of Δm and m_t were used. Specific heat which actually is not constant, was evaluated at the arithmetic mean temperature,

$$T_M = \frac{1}{2}(T_i + T_s) \tag{26}$$

This based specific heat on readily available temperatures.

Experimental gas phase data was used to obtain ΔH by numerical integration of gas density and specific enthalpy profiles according to

$$\Delta H = \int_o^{V_f} h_f \rho_f \, dV - \int_o^{V_o} h_o \rho_o \, dV \tag{27}$$

Gas densities were obtained as indicated previously in the mass transfer calculation. Specific enthalpy data were obtained from reference 5 for hydrogen and reference 6 for helium.

The comparison of these two methods for evaluating enthalpy change is shown in columns 8 through 10 in table 1. The agreement is seen to be good, with a maximum deviation of -6.74% and average deviation of -2.79%. This indicates that the assumptions made in the derivation of equation (16) and the evaluation of the specific heat at temperature T_M did not introduce an appreciable error in determining ΔH for the 10 test runs.

HEAT TRANSFER. The heat transferred from the gas phase during the liquid discharge period Q was calculated from equation (6) by substituting experimentally determined values of ΔH, Δm, and m_t. These values of total heat transfer are listed in column 11 of table 1.

DISTRIBUTION. In order to obtain an indication of the distribution of the total heat transfer, estimates were made of the heat input to the tank wall, Q_w, and the tank end region, Q_e. The end region heat transfer included the heat inputs to the dome, diffuser, and piping. End region heat input was computed in two ways: from the specific heats, masses, and measured temperature rises of the respective components; and from the drop in enthalpy of the inlet gas due to its temperature change between the inlet pipe and the lower diffuser screen. Results of both methods checked fairly well, and values obtained from the former method are listed in column 12 of table 1. The tank heat input Q_e is a small term which does not vary greatly. An average value of 130 Btu was indicated for the test runs.

The heat input to the tank wall was calculated from the mass, specific heats, and measured temperature rises of the wall. In order to properly account for longitudinal temperature variation, the wall was divided into 20 cylindrical shell volume elements, and the heat input to each summed. These values of Q_w are tabulated in column 13 of table 1.

The sum of Q_w and Q_e obtained in this manner was then compared to the total heat transfer Q obtained from the energy balance. Deviation varied from 13.7 to 30.8%, with Q always greater. It is believed that this discrepancy is due primarily to possible inaccuracies in the calculation of the wall heat transfer. The prime source of inaccuracy here may be in the uncertainty of the data used for specific heat of stainless steel.* A second possible source of inaccuracy may have been due to the existence of temperature gradients across the tank wall due to the transient heating of the walls (wall temperature measurements were made on the outer surface of the wall). However, preliminary calculations indicate that these transient gradients are minor.

In view of the uncertainty in the calculated wall heat transfer, it was decided to use the difference $Q - Q_e$ for Q_w. These values are listed in column 14 of table 1. It is seen that wall heat transfer increases with increased tank pressure and discharge time, and was approximately the same for hydrogen and helium.

It is valuable to compare the heat the wall receives from the gas with that it receives from the ambient surroundings via heat leak through the vacuum jacket. A good average for gas-wall heat flux was 2000 Btu/(hr)(sq ft), whereas ambient-wall heat flux was only about 40 Btu/(hr)(sq ft). This indicates that ambient heat leak is negligibly low.

*Experimental information is scarce for temperatures below room temperature. The data used in this report (obtained from ref. 7) were calculated from the Debye equation on the basis of 18% chromium, 8% nickel, the balance γ-Fe and then adjusted for agreement with experimental values near room temperature. Thus the specific heat data are based on a theoretical equation the results of which are weight averaged.

CORRELATION OF WALL HEAT TRANSFER. Evaluation of the parameters of equation (23) required the determination of C, C_w, and $\mathcal{N}$. For simplicity, the gas properties $\overline{C}_p$ and $\overline{\rho}$ in C were evaluated at the mean temperature as defined in equation (26). The mean wall specific heat in C_w was evaluated as

$$\overline{C}_{p,w} = \frac{1}{T_i - T_s} \int_{T_s}^{T_i} C_{p,w}\, dT \tag{28}$$

An overall heat transfer coefficient for each discharge was calculated from the standard correlation for vertical free convection (ref. 8).

$$\frac{\mathcal{N}L}{k} = 0.13 \left[\left(\frac{L^3 \rho^2 g\beta\, \Delta T}{\mu^2} \right) \left(\frac{C_p M}{k} \right) \right]^{1/3} \tag{29}$$

For equation (29), all gas properties were evaluated at the mean temperature defined by equation (26). Also, since $\mathcal{N}$ is not particularly sensitive to ΔT, it was found sufficient to use an average value of ΔT for all the runs. This value was 175° R which represents a value of $\Delta T/(T_i - T_s)$ of approximately 0.375. Comparison between these calculated heat transfer coefficients and experimentally determined values showed fair agreement as indicated in columns 15, 16, and 17 of table 1.

Values of the dimensionless groups used in the correlation are given in columns 18, 19, and 20 of table 1. As L/D was essentially constant at a value of 2.5, its effect on heat transfer could not be experimentally correlated. The correlation is presented as a plot of $\left(\frac{Q_w}{Q_{w,\infty}}\right) \Big/ \left(\frac{\mathcal{N}\theta}{C_w}\right)^{0.55}$ versus $\left(\frac{C}{C_w}\right)$ as shown in Figure 5.

As extensive data were not taken and the individual effects of all the variables not studied, this correlation should be viewed as a tentative result. Also, for these reasons, no attempt was made to mathematically represent the

faired curve. The limitations of the correlation are implied in table 2 which lists the range of each of the variables studied.

COMPARISON OF TERMS. The dependance of gas usage on the processes occurring during discharge is expressed by equation (24). The portion of the total gas usage attributable to each term within the bracket of equation (24) was determined by dividing each term by the common factor $[(h_i - h_s) + C_p T_s]$. These quantities (units of mass) are tabulated in columns 21 through 24 of table 1.

It is clear from this comparison that: (1) the major contributants to gas usage are the displacement and wall heat transfer terms; (2) the end heat transfer is a small effect which makes its largest contribution for low pressure, rapid discharges; and (3) the effect of the interfacial mass transfer term may be neglected.

Prediction of Gas Requirements

Using equation (24), the experimental discharge conditions, and the methods of calculation and prediction herein developed, gas requirements Δm were calculated. The procedure involved for a given P, ΔV, θ, T_i, T_s, and pressurant was as follows:

(1) The specific enthalpies, h_i and h_s, were obtained from T_i, T_s, P and the data of references 6 and 7.

(2) All gas properties were evaluated at the average temperature between T_i and T_s.

(3) Wall heat capacity and maximum heat addition were computed from equations (28) and (22) respectively.

(4) Gas to wall temperature drop in equation (29) was estimated from $\Delta T/(T_i - T_s) = 0.375$.

(5) The groups $(\Delta\theta/C_w)$ and (C/C_w) were computed and Φ obtained from the correlation of Figure 5.

(6) A value of 130 Btu was used for Q_e.

(7) Gas usage, Δm, is then calculated from equation (24).

Predicted values of gas requirement were calculated according to this procedure for the ten test runs and compared with experimental values as determined from the gas supply cylinders. These results are shown in columns 25 through 27 of table 1. Deviation was 4.48% on the average and 14.0% maximum.

In using the method proposed herein to predict gas requirements under conditions other than those studied in this report, the following problems and limitations should be noted:

(1) Tank movement, particularly oscillation, may disturb the gas liquid interface sufficiently to cause significant mass transfer.

(2) The tentative heat transfer correlation is based upon data limited both in quantity and in the range of operating conditions studied. Furthermore test conditions such as inlet gas temperature, wall material, heat leak and tank geometry were not varied.

(3) End heat transfer will differ from system to system depending upon such variables as diffuser design and dome geometry. In order to facilitate analysis, the tank used in this study was designed to minimize end heat transfer. However in a realistic system, end heat transfer could well be important, and therefore warrants consideration.

The proposed prediction method, while restricted in its ability to quantitatively predict gas requirements, can be very helpful in qualitatively analyzing the effects of system parameters. To facilitate qualitative study, equation (24) was simplified by: (1) dropping the small terms (mass transfer

and end heat transfer); (2) substituting into it the approximate relationship for h_i

$$h_i \approx h_s + C_p(T_i - T_s) \tag{30}$$

and algebraically simplifying; and (3) substituting into it the wall heat transfer correlation

$$Q_w = Q_{w,\infty} \left(\frac{\mathcal{H}\theta}{C_w}\right)^{0.55} \Phi' \left(\frac{C}{C_w}\right) \tag{31}$$

These changes yielded

$$\Delta m \approx \frac{(M/R)P\ \Delta V}{T_i} + \frac{Q_{w,\infty}(\mathcal{H}\theta/C_w)^{0.55}\Phi'(C/C_w)}{C_p T_i} \tag{32}$$

For instance, the effect of choice of pressurant on gas requirements can be seen. As helium's molecular weight is twice that of hydrogen (M is about 4 for helium and 2 for hydrogen), the displacement term $[(M/R)P\ \Delta V/T_i]$ for helium pressurant is twice that for hydrogen pressurant at the same inlet temperature. For the wall heat transfer term, the main difference is due to effect of specific heat, C_p. Helium's specific heat is about 1.25 Btu/lb-mass $^{\circ}R$, hydrogen's is about 3.05 Btu/lb-mass $^{\circ}R$. It should be noted that neither the product $\bar{C}_p\bar{\rho}D$ comprising C, nor the heat transfer coefficient in the group $(\mathcal{H}\theta/C_w)$ have significantly different values for helium than for hydrogen. Thus the wall heat transfer term is about 2.4 times as large for helium than for hydrogen pressurant. Experimental results (see table 1) revealed that about twice as much helium as hydrogen was needed for a given discharge, which agrees with the qualitative analysis described above.

The effects of other variables, e.g., inlet gas temperature and tank pressure can be similarly investigated by analysis of equation (32).

Summary

An analytical relation has been developed expressing gas requirements for the pressurized transfer of liquid hydrogen from a cylindrical tank as a function of known system parameters and two quantities to be experimentally determined, i.e., interfacial mass transfer and gas phase heat transfer. For the experimental test conditions studied (in particular, a quiescent gas-liquid interface and low heat leak from the ambient) the effect of mass transfer on gas requirements was found to be negligibly small. The heat transferred to the wall, which constituted the major contributant to gas phase heat transfer, was predicted by a correlation developed herein with reasonable certainty within the range of the experimental test conditions considered.

From the analytical relation and the generalization of the experimental results, gas requirements were predicted with reasonable accuracy for the experimental test conditions. Furthermore, the effect of system parameters on gas requirements could be qualitatively estimated from an approximate relation derived from the analysis.

Nomenclature

C	thermal capacity, Btu/(sq ft)($^{\circ}$R)
C_p	specific heat at constant pressure, Btu/(lb mass)($^{\circ}$R)
D	tank inner wall diameter, ft
g	local gravitational acceleration, ft/sec^2
H	enthalpy of gas phase at any time, Btu
ΔH	enthalpy change of gas phase during discharge, Btu
$\mathcal{H}$	average heat transfer coefficient between gas and wall, Btu/(hr)(sq ft)($^{\circ}$R)
h	specific enthalpy of gas, Btu/lb mass

J	Joule's constant, 778 ft-lb force/Btu
k	thermal conductivity of gas, Btu/(hr)(sq ft)(^{o}R)
L	length discharged, ft
M	molecular weight, lb mass/lb mole
m	mass of gas phase, lb mass
Δm	mass of pressurant required for discharge, lb mass
P	tank pressure, lb force/(sq in.)
Q	heat transferred from the gas phase during discharge, Btu
$Q_{w,\infty}$	heat transferred to the tank wall if wall heats to temperature of inlet pressurant, Btu
R	gas law constant, (lb force/sq in.)(cu ft)/(lb mole)(^{o}R)
T	gas or wall temperature, ^{o}R
ΔT	temperature driving force for heat transfer, ^{o}R
U	internal energy of gas phase, Btu
V	volume of gas phase at any time, cu ft
ΔV	volume change of gas phase during discharge, cu ft
β	thermal coefficient of expansion, $^{o}R^{-1}$
δ	wall thickness, ft
θ	discharge time, hr
μ	viscosity of gas, lb mass/(ft)(sec)
π	geometric constant
ρ	density of gas, lb mass/cu ft
ρ_w	density of wall, lb mass/cu ft
Φ, Φ'	express functional relations
φ	time, hr

Subscripts:

e tank end

f final gas state, at end of discharge

i state of inlet gas

M arithmetic mean

o original gas state, at start of discharge

R reference value

s saturated condition at pressure P

t transferred at interface

w tank wall

Superscript:

$\bar{}$ mean value

References

1. J. A. Clark, S. K. Fenster, H. Merte, Jr., and W. A. Warren: Pressurization of Liquid Oxygen Containers, University of Michigan, Engineering Research Institute, Report 2646-9-P, June 1958.

2. J. A. Clark, V. S. Arpaci, and W. O. Winer: Dynamic Response of Fluid and Wall Temperatures During Pressurized Discharge of a Liquid From a Container. Advances in Cryogenic Engineering, volume 6, pp. 310-322, Plenum Press, 1960.

3. C. A. Herr et al.: Suitability of Carbon Resistors for Field Measurements of Temperatures in the Range 35° to 100° R. NASA TN D-264, February, 1960.

4. Harold W. Wooley, Russell B. Scott, and F. G. Brickwedde: Compilation of Thermal Properties of Hydrogen in its Various Isotopic and Ortho-Para Modifications, RP1932, Journal of Research of the National Bureau of Standards, vol. 41, Nov. 1948.

5. Temperature-Entropy Diagrams for Hydrogen. (Unpublished) Lewis Research Center, NASA.

6. Jesse T. Simmons: The Physical and Thermodynamic Properties of Helium, Wm. R. Whittaker Co., Ltd., Technical Report D-9027, July 1957.

7. Russell B. Scott: Cryogenic Engineering, D. Van Nostrand Company, Inc., Princeton, New Jersey.

8. W. H. McAdams: Heat Transmission, Third Edition, p. 172, McGraw-Hill, New York, 1954.

TABLE 1. - MAJOR RESULTS

1	2	3	4	5	6	7	8	9	10	11	12	13	14
Run	Pressurant	Discharge pressure, P, lb-F/in.^{2}	Discharge time, θ, sec	Volume discharged, ΔV, ft^3	Temperature of inlet gas, T_i, $^\circ R$	Percent mass transferred, $m_t/\Delta m$, %	Gas phase enthalpy change, ΔH			Heat transferred as calculated from Eq. (6), Q, Btu	End heat transfer, Q_e, Btu	Wall heat transfer as calculated from temperature rise of wall, Q_w, Btu	Wall heat transfer as calculated from $(Q - Q_e)$, Q_w, Btu
							Theoretical, Btu	Actual, Btu	Deviation based on actual, %				
1	Hydrogen	160.0	338.2	22.6	506	-1.23	2524	2613	3.41	3998	149	3303	3849
2	Hydrogen	161.2	87.5	20.9	517	-0.71	2240	2272	1.41	2153	146	1463	2007
3	Hydrogen	160.7	98.9	22.6	530	-7.77	2462	2452	-0.41	2384	103	1547	2281
4	Hydrogen	57.0	310.7	23.5	513	-3.30	1108	1038	-6.74	2202	117	1617	2085
5	Hydrogen	58.1	113.0	24.8	520	-0.73	1038	1003	-3.49	1389	148	859	1241
6	Helium	159.6	366.1	22.9	527	12.0	1711	1639	-4.21	4013	113	3089	3900
7	Helium	159.8	87.3	23.0	525	-4.46	1710	1793	4.63	1791	91	1268	1700
8	Helium	57.5	333.1	22.9	534	9.07	601	582	-2.23	2202	133	1636	2069
9	Helium	55.7	93.0	22.4	505	0.56	586	579	-1.21	994	146	620	848
10	Helium	58.0	94.9	22.9	525	-0.60	623	624	0.16	1111	138	706	973

15	16	17	18	19	20	21	22	23	24	25	26	27
Heat transfer coefficient, $\mathcal{H}$			Dimensionless ratios			Mass terms, equation (24)				Prediction of gas requirements, Δm		
Calculated from natural convection correlation, Btu/hr-ft^2-$^\circ R$	Experimental average for discharge, Btu/hr-ft^2-$^\circ R$	Deviation based on calculated coefficient, %	Wall heat transfer number $Q_w/Q_{w,\infty}$	Thermal capacity ratio number, C/C_w	Wall response number, $h\theta/C_w$	Mass required due to displacement, lb-mass	Mass required due to mass transfer, lb-mass	Mass required due to wall heat transfer, lb-mass	Mass required due to end heat transfer, lb-mass	Experimentally measured gas requirements, lb-mass	Predicted gas requirements, lb-mass	Deviation based on measured requirements, %
17.9	14.9	19.8	0.187	0.754	1.432	1.308	-0.005	2.421	0.094	3.875	3.865	0.26
17.8	14.8	20.7	.103	.733	.357	1.196	-0.002	1.234	.080	2.540	2.465	2.95
17.7	13.5	31.2	.103	.714	.368	1.276	-0.022	1.367	.062	2.712	2.878	-6.12
9.0	8.4	7.28	.0922	.257	.711	.475	-0.005	1.192	.073	1.875	1.908	-1.49
9.0	8.6	5.24	.0540	.265	.272	.508	-0.001	.783	.093	1.363	1.417	-3.96
12.6	13.1	-4.11	.184	.526	1.387	2.593	.112	5.936	.172	8.591	8.529	.72
12.4	12.6	-1.51	.0773	.508	.305	2.605	-0.025	2.595	.139	5.468	5.565	-1.77
6.0	8.3	-27.1	.0942	.211	.786	.898	.032	3.120	.201	4.194	3.612	14.00
6.6	8.2	-19.5	.0422	.222	.219	.928	.001	1.352	.233	2.505	2.328	7.07
6.5	7.8	-17.1	.0453	.221	.213	.951	-0.001	1.494	.212	2.662	2.490	6.46

TABLE 2. - RANGE OF PARAMETERS AND GROUPS FOR WALL HEAT TRANSFER CORRELATION

PARAMETER OR GROUP	RANGE	VARIATION
C, BTU/($^{\circ}$R)(SQ FT)	0.206 - 0.739	3.59 FOLD
C_W, BTU/($^{\circ}$R)(SQ FT)	0.958 - 1.019	ESSENTIALLY CONSTANT
$\mathcal{H}$, BTU/(HR)(SQ FT)($^{\circ}$R)	8.15 - 14.94	1.83 FOLD
θ, HR	0.0242 - 0.102	4.21 FOLD
D, FT	2.26	CONSTANT
Q_W, BTU	848 - 3900	4.59 FOLD
$Q_{W,\infty}$, BTU	19,500 - 23,000	ESSENTIALLY CONSTANT
L/D, DIMENSIONLESS	2.32 - 2.65	ESSENTIALLY CONSTANT
C/C_W, DIMENSIONLESS	0.211 - 0.754	3.57 FOLD
$\mathcal{H}\theta/C_W$, DIMENSIONLESS	0.213 - 1.432	6.72 FOLD
$Q_W/Q_{W,\infty}$, DIMENSIONLESS	0.0422 - 0.187	4.43 FOLD

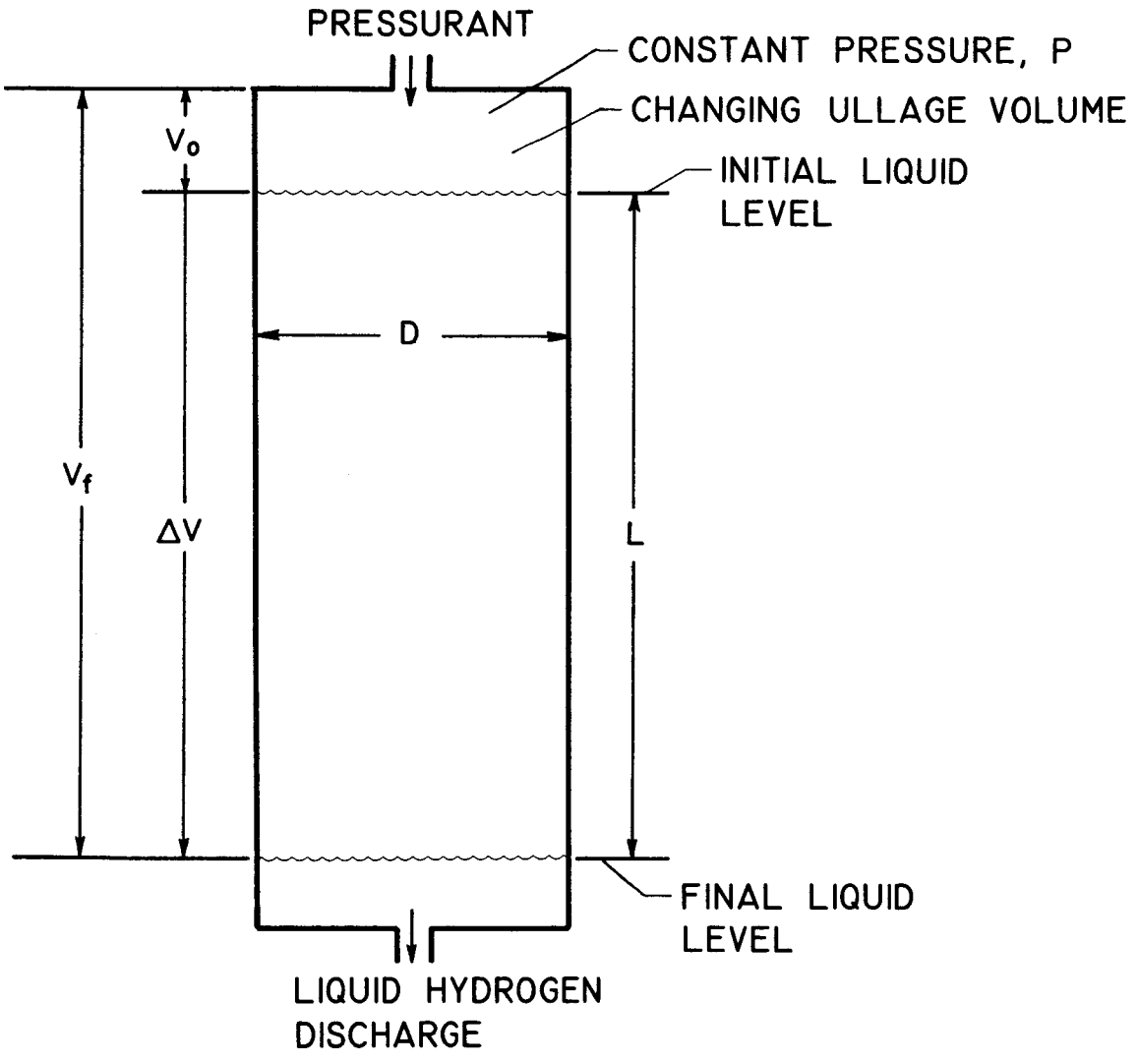

Figure 1. - Schematic of tank discharge.

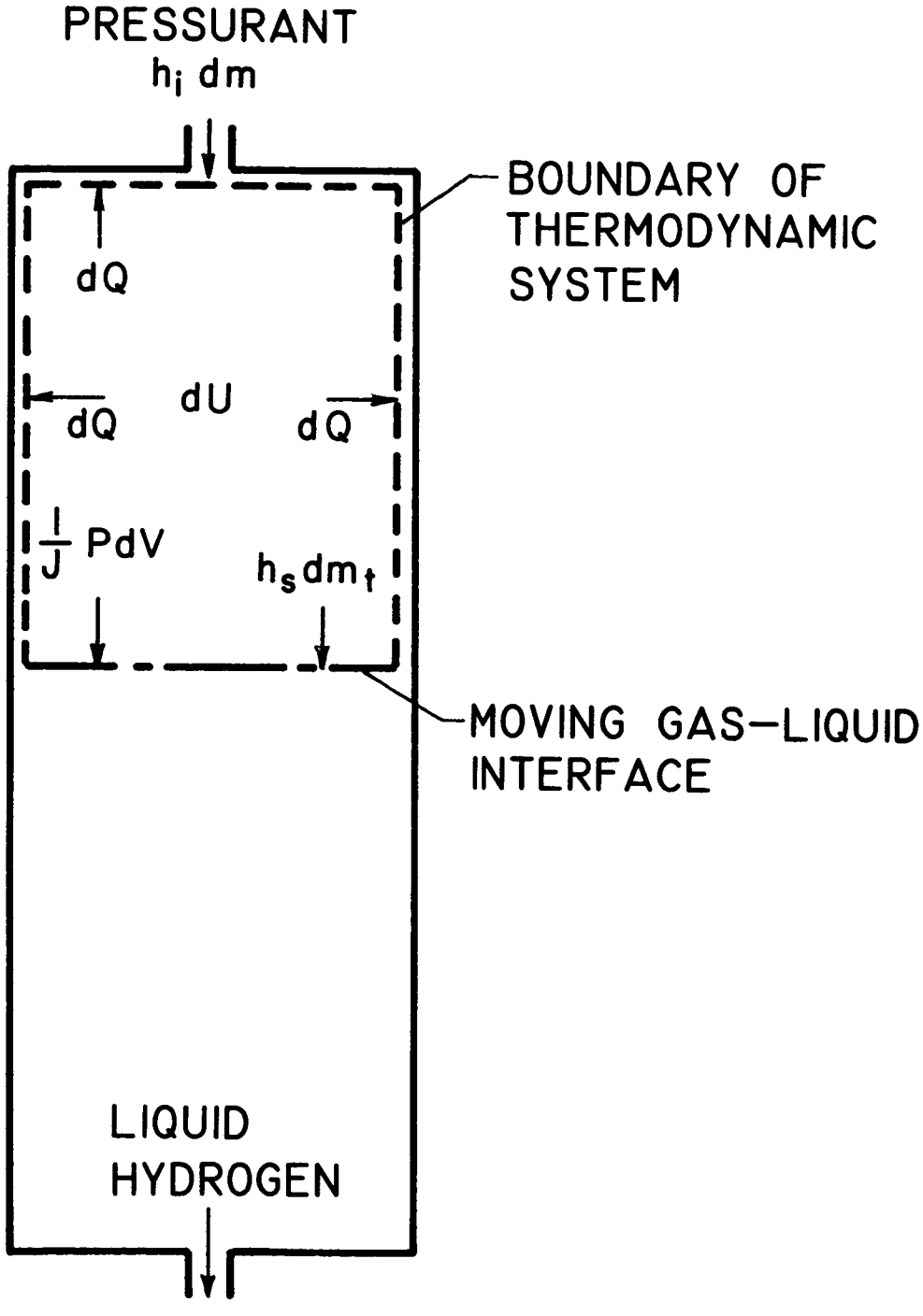

Figure 2. - Schematic of energy processes during tank discharge.

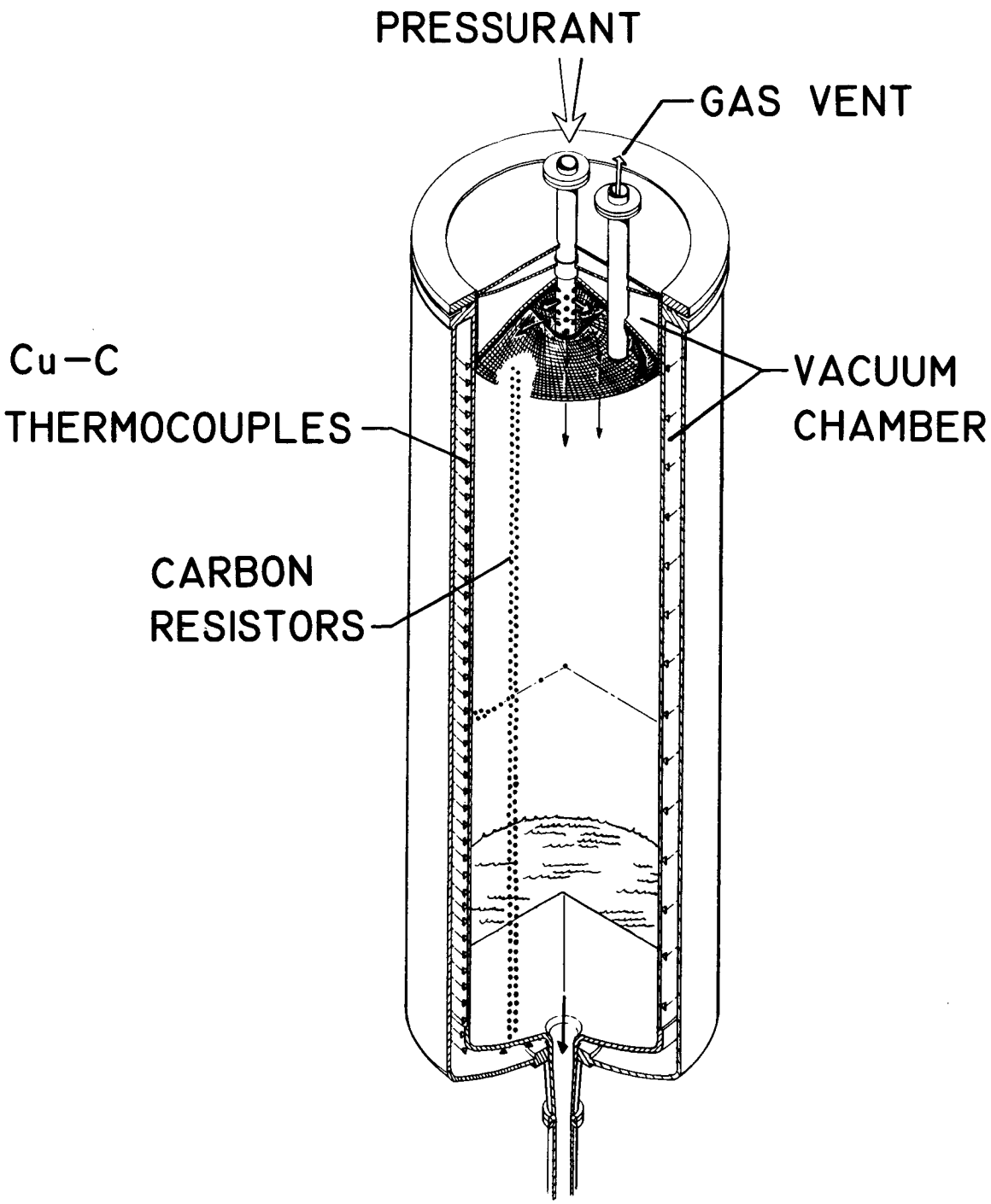

Figure 3. - Tank and instrumentation.

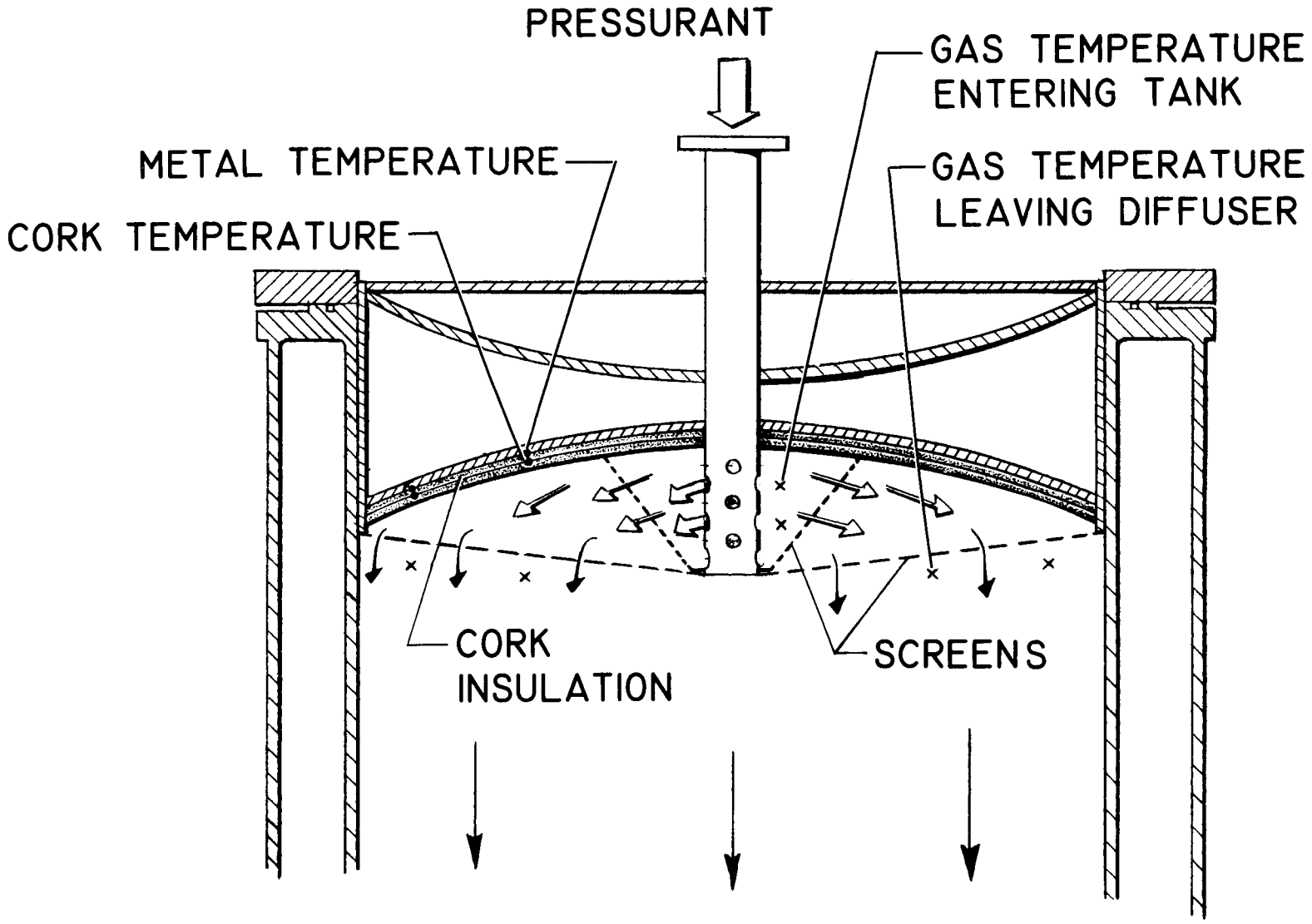

Figure 4. - Diffuser and instrumentation.

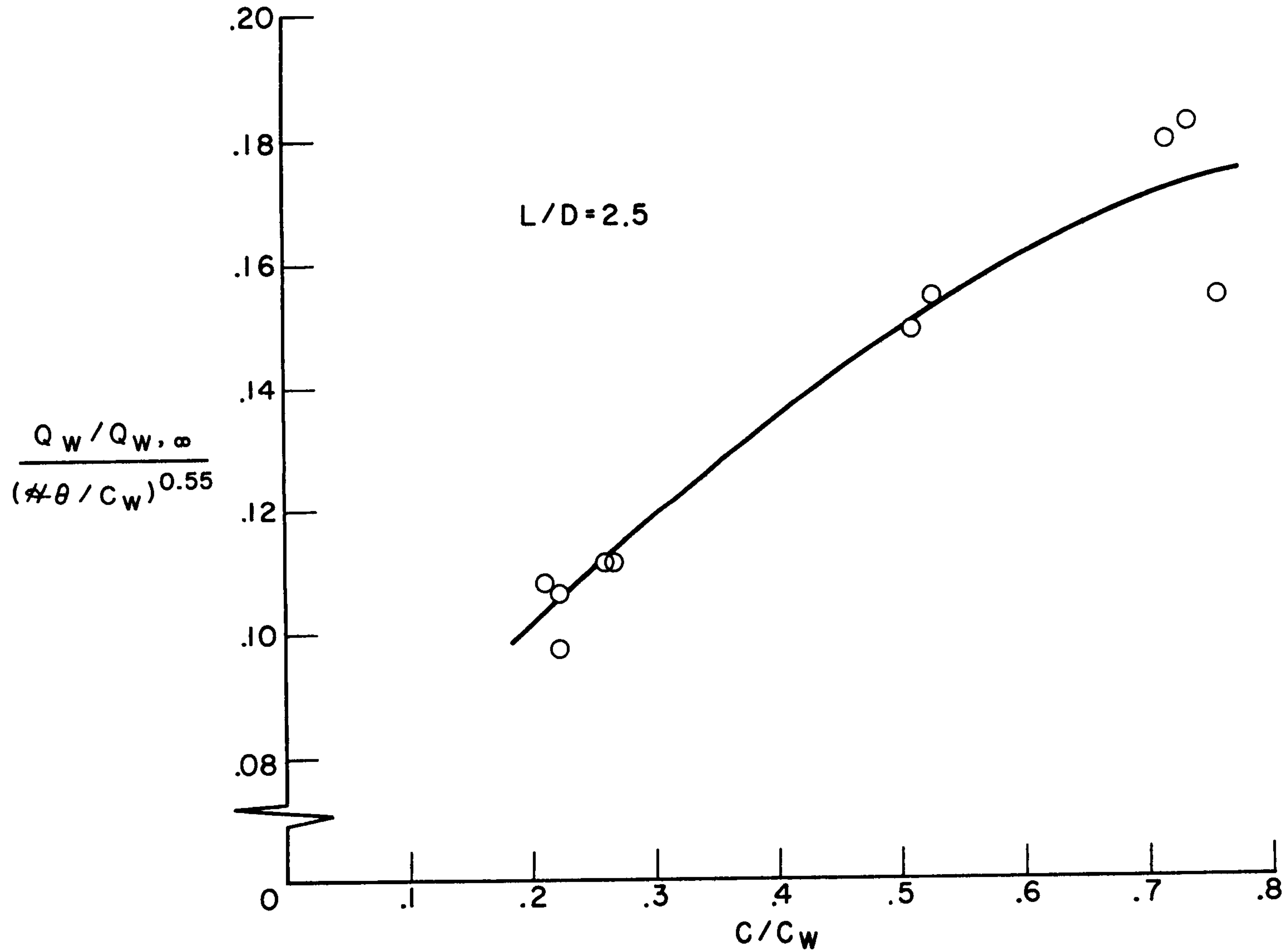

Figure 5. - Wall heat transfer correlation.